

## Kinematically Consistent Velocity Fields for Hydrodynamic Calculations in Curvilinear Coordinates

E. M. PARMENTIER

*Department of Geological Sciences*

AND

K. E. TORRANCE

*Sibley School of Mechanical and Aerospace Engineering,  
Cornell University, Ithaca, New York 14853*

Received June 17, 1974; revised June 3, 1975

Kinematically consistent velocities are derived for use with finite difference hydrodynamic calculations in cylindrical coordinates. The velocities satisfy mass conservation and the circulation theorem both locally and globally. When combined with a conserving finite difference form of the hydrodynamic transport equations using vorticity-streamfunction variables, a fully conserving difference approximation results. An illustrative example involving thermal convection of an infinite Prandtl number, variable viscosity fluid is presented. Kinematically consistent velocities are found to be essential for obtaining solutions free from physical anomalies. The approach is readily generalized to other curvilinear coordinate systems.

### INTRODUCTION

The desirability of using conserving difference approximations for the hydrodynamic transport equations has long been recognized (Fromm [1]). In Cartesian coordinates, it is relatively simple to construct difference approximations that conserve mass, vorticity, and energy. However, in curvilinear coordinates this is more difficult to achieve. Two separate aspects must be considered: conservation of thermal energy and vorticity by the transport equations, and conservation of mass. The first aspect has been adequately discussed in the literature and conserving difference approximations for curvilinear coordinates are available. However, the second aspect has not been treated fully and it forms the subject of the present paper. The velocity fields used for a streamfunction-vorticity formulation of the hydrodynamic equations must not only conserve mass, but they must also satisfy the circulation theorem. In this paper, new finite difference approximations for

velocity fields are developed that satisfy the kinematic constraints imposed by conservation of mass and the circulation theorem (kinematically consistent velocities). Although formulated here in cylindrical coordinates, the approach is applicable to any curvilinear coordinate system.

The physical problem that motivated the present study is that of steady-state thermal convection in the Earth's mantle. The problem is for a large Prandtl number and a variable viscosity, which depends strongly on temperature and depth. Recent studies of variable viscosity convection include those of Turcotte *et al.* [7], Liang *et al.* [3], and Houston and DeBraemaker [2]. We have found that the use of currently available differencing techniques to obtain velocity fields resulted in physically anomalous flows for the present problem. The anomalies were eliminated by the use of kinematically consistent velocity fields. Application of the present method to a range of parameters representative of mantle convection is reported by Parmentier *et al.* [5].

MATHEMATICAL FORMULATION

We will consider the axisymmetric motion of a viscous incompressible fluid in a cylindrical enclosure. The origin of the  $(x, r)$  coordinate system is at the center of the circular base. Velocity components in the axial and radial directions are denoted by  $u$  and  $v$ . With the Boussinesq approximation, the governing equations become

$$\frac{\partial u}{\partial x} + \frac{1}{r} \frac{\partial}{\partial r} (rv) = 0 \tag{1}$$

$$\frac{\partial \theta}{\partial t} + \frac{\partial}{\partial x} (u\theta) + \frac{1}{r} \frac{\partial}{\partial r} (rv\theta) = \nabla^2 \theta \tag{2}$$

$$\begin{aligned} \frac{1}{Pr} \left[ \frac{\partial \zeta}{\partial t} + \frac{\partial}{\partial x} (u\zeta) + \frac{\partial}{\partial r} (v\zeta) \right] = & -Ra \frac{\partial \theta}{\partial r} + \frac{1}{r} D^2(rv\zeta) \\ & - 2 \left[ \frac{\partial v}{\partial x} \frac{\partial^2 v}{\partial r^2} - \frac{\partial u}{\partial r} \frac{\partial^2 v}{\partial x^2} + \frac{\partial^2 v}{\partial x \partial r} \left( \frac{\partial u}{\partial x} - \frac{\partial v}{\partial r} \right) \right] \end{aligned} \tag{3}$$

$$\zeta = \frac{\partial v}{\partial x} - \frac{\partial u}{\partial r} \tag{4}$$

where

$$\nabla^2 = \frac{1}{r} \frac{\partial}{\partial r} \left( r \frac{\partial}{\partial r} \right) + \frac{\partial^2}{\partial x^2}$$

and

$$D^2 = r \frac{\partial}{\partial r} \left( \frac{1}{r} \frac{\partial}{\partial r} \right) + \frac{\partial^2}{\partial x^2}.$$

The various equations are respectively the continuity equation, the transport equations for temperature ( $\theta$ ), and azimuthal vorticity ( $\zeta$ ), and the vorticity definition. The quantity  $\nu$  is a normalized kinematic viscosity, and gravity ( $g$ ) is directed along the negative  $x$ -axis.

A streamfunction ( $\psi$ ) is introduced by defining

$$u = (1/r)(\partial\psi/\partial r) \quad (5a)$$

$$v = -(1/r)(\partial\psi/\partial x). \quad (5b)$$

The continuity equation is then satisfied identically. Introducing the streamfunction definitions (5) into the vorticity definition (4) gives the streamfield equation

$$D^2\psi = -r\zeta. \quad (6)$$

Eqs. (5) and (6) replace Eqs. (1) and (4).

The foregoing equations are written in nondimensional form using the enclosure height ( $h$ ) as the length scale, the ratio  $h^2/\kappa$ , (where  $\kappa$  is the thermal diffusivity) as the time scale, and a characteristic temperature difference  $\Delta T$ , as the temperature scale. The Raleigh and Prandtl numbers emerge as dimensionless, physical parameters:

$$Ra = \frac{\alpha g h^3 \Delta T}{\nu_0 \kappa}$$

$$Pr = \frac{\nu_0}{\kappa},$$

where  $\alpha$  is the volume thermal expansion coefficient and  $\nu_0$  is a reference value of the kinematic viscosity.

#### CONSERVING FINITE DIFFERENCE APPROXIMATIONS AND THE CIRCULATION THEOREM

The transport equations (2) and (3) express local conservation of thermal energy and vorticity. The energy equation conserves thermal energy in an infinitesimal volume element ( $dV = 2\pi r dr dx$ ), and the vorticity equation conserves vorticity for an infinitesimal area element in the  $x - r$  plane ( $dA = dx dr$ ). In differential form the equations may be integrated to give global conservation equations for a prescribed region in space. If the finite difference forms of the transport equations satisfy local conservation on a grid volume, the difference approximations are called conserving. They can then be integrated or summed over the mesh without introducing spurious sources or sinks for the transported variables. Conserving difference approximations in cylindrical coordinates have been discussed by Torrance [6].

Conserving approximation of the convection terms requires the introduction of transport velocities. Consider the element of area shown in Fig. 1, which

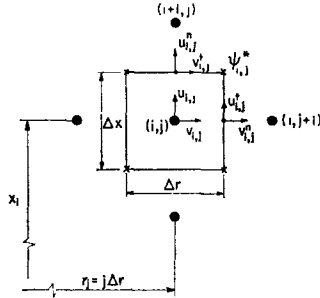


FIG. 1. Notation for an interior gridpoint of a uniform spatial mesh in cylindrical coordinates. The grid volume is centered on the gridpoint.

encloses a gridpoint  $(i, j)$ . The faces of this grid volume are located midway between adjacent gridpoints. The transport velocities, denoted by  $(u_{i,j}^n, v_{i,j}^n)$ , represent the volume flow through the faces of the grid volume and so are used to approximate the convective flux of transported quantities. Also shown in Fig. 1 are gridpoint velocities  $(u_{i,j}, v_{i,j})$ . Torrance [6] calculated gridpoint velocities from the streamfunction field by central difference approximations to Eq. (5):

$$u_{i,j} = (\psi_{i,j+1} - \psi_{i,j-1})/2r_j \Delta r \tag{7a}$$

$$v_{i,j} = -(\psi_{i+1,j} - \psi_{i-1,j})/2r_j \Delta x. \tag{7b}$$

The streamfield equation (6) was also approximated by central differences. Transport velocities were defined by spatial interpolation of the gridpoint velocities

$$u_{i,j}^n = (u_{i,j} + u_{i+1,j})/2 \tag{8a}$$

$$v_{i,j}^n = (v_{i,j} + v_{i,j+1})/2. \tag{8b}$$

For an incompressible fluid, the transport velocities should conserve volume flow on the grid volume over which other transported variables are conserved. It can be shown that the transport velocities defined above conserve volume flow in Cartesian coordinates. If conservation is not satisfied a spurious volume source  $Q_{i,j}$  is introduced in the grid volume. In cylindrical coordinates the volume source (in units of fluid volume produced per unit volume and time) is given by a flux balance as

$$Q_{i,j} = [u_{i,j}^n - u_{i-1,j}^n]/\Delta x + [v_{i,j}^n(r_j + (\Delta r/2)) - v_{i,j-1}^n(r_j - (\Delta r/2))]/r_j \Delta r. \tag{9}$$

Substituting (8) into (9) reveals a spurious volume source for interior grid volumes. The volume source can also be written

$$Q_{i,j} = \frac{1}{2} \left( \frac{\Delta r}{r_j} \right)^2 \left( \frac{\partial v}{\partial r} \right)_{i,j} - \frac{(\Delta r)^2}{4r_j} \left( \frac{\partial^2 v}{\partial r^2} \right)_{i,j} + \dots \quad (10)$$

for small  $\Delta x$ ,  $\Delta r$ , and  $\Delta r/r_j$ . This equation indicates that the volume source is strongest near the axis and in regions of large velocity gradients. In the limit  $\Delta r \rightarrow 0$ , the volume source vanishes.

The failure of transport velocities to conserve volume flow has led us to reconsider the formulation of finite difference approximations for velocities in cylindrical coordinates. In addition to conserving volume flow, velocities should satisfy the circulation theorem both locally and globally. The circulation theorem can be written

$$\int_A \zeta \, dA = \oint \mathbf{v} \cdot d\mathbf{l}, \quad (11)$$

where  $A$  and  $l$  are the area and perimeter of the region of integration in the  $x - r$  plane. The differential form of the vorticity definition satisfies the circulation theorem identically. The finite difference approximations for velocity and vorticity fields should do so as well. Since the conditions imposed by volume flow conservation and the circulation theorem are kinematic in nature, we will refer to velocity fields that satisfy these conditions as kinematically consistent velocities.

### KINEMATICALLY CONSISTENT VELOCITY FIELDS

Consider again the incremental volume of cross-sectional area  $\Delta x \Delta r$  containing the gridpoint  $(i, j)$  in Fig. 1. We begin by defining internodal velocities on the faces of the grid volume. The normal and tangential components of velocity are denoted by superscripts. The pair  $(u_{i,j}^n, v_{i,j}^t)$  is on the  $i + 1/2$  face while the pair  $(u_{i,j}^t, v_{i,j}^n)$  is on the  $j + 1/2$  face.

#### *Tangential Velocity Components and the Circulation Theorem*

We first consider the circulation theorem (11) and the relationship between vorticity and tangential velocity components that it implies. Approximation of the integrals leads to the following expression for the area-averaged value of vorticity in the grid volume

$$\zeta_{i,j} = [(v_{i,j}^t - v_{i-1,j}^t) \Delta r - (u_{i,j}^t - u_{i,j-1}^t) \Delta x] / \Delta x \Delta r. \quad (12)$$

The area-averaged value is assigned to the gridpoint  $(i, j)$ . This can also be recognized as a central difference approximation to Eq. (4).

The circulation theorem may also be applied to half-size grid volumes adjacent to the boundaries. Adjacent to a solid boundary such as  $x = 0$  (Fig. 2a), the circulation theorem gives

$$\zeta_{0,j} = 2[(v_{0,j}^t - v_{0,j}) \Delta r - (u_{0,j}^t - u_{0,j-1}^t)(\Delta x/2)]/\Delta x \Delta r, \tag{13}$$

whereas along the axis  $r = 0$  (Fig. 2b),

$$\zeta_{i,0} = 2[(v_{i,0}^t - v_{i-1,0}^t)(\Delta r/2) - (u_{i,0}^t - u_{i,0}) \Delta x]/\Delta x \Delta r. \tag{14}$$

The boundary velocities  $u_{i,0}$  and  $v_{0,j}$  appear in the last two equations.

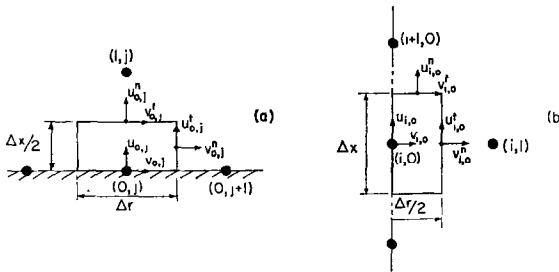


FIG. 2. Notation for boundary gridpoints. (a) At  $x = 0$  boundary. (b) On the axis.

Equations (12)–(14) are based on the circulation theorem and define difference approximations for the area-averaged vorticity for all grid volumes in a cylindrical region. Note that it is the area-averaged vorticity which is conserved by the vorticity transport equation. The formal accuracy of the expressions is second order. When appropriately defined tangential velocities are introduced into the equations, the circulation theorem will be satisfied globally because the contributions to the line integral of Eq. (11) from adjacent elements, cancel along all common boundaries.

Since the faces of grid volumes are midway between mesh points of the grid, approximations for the tangential velocities in terms of streamfunction may be obtained from Eq. (5) as

$$u_{i,j}^t = (\psi_{i,j+1} - \psi_{i,j})/(r_j + (\Delta r/2)) \Delta r \tag{15a}$$

$$v_{i,j}^t = -(\psi_{i+1,j} - \psi_{i,j})/r_j \Delta x. \tag{15b}$$

Velocities at gridpoints are found by linear interpolation of the tangential velocities; on a uniform mesh

$$u_{i,j} = (u_{i,j}^t + u_{i,j-1}^t)/2 \quad (16a)$$

$$v_{i,j} = (v_{i,j}^t + v_{i-1,j}^t)/2. \quad (16b)$$

This approach for defining gridpoint velocities was used by Fromm [1] in Cartesian coordinates. In Cartesian coordinates, it is equivalent to the central differences in Eq. (7). Note that this is not true in cylindrical coordinates.

For interior gridpoints, application of the circulation theorem (12) and Eq. (15) gives the conventional central difference form of the streamfield equation

$$\begin{aligned} & [\psi_{i+1,j} - 2\psi_{i,j} + \psi_{i-1,j}]/(\Delta x)^2 + [(j/(j + \frac{1}{2}))(\psi_{i,j+1} - \psi_{i,j}) \\ & - (j/(j - \frac{1}{2}))(\psi_{i,j} - \psi_{i,j-1})]/(\Delta r)^2 = -j \Delta r \zeta_{i,j}. \end{aligned} \quad (17)$$

If gridpoint velocities defined by Eq. (7) are linearly interpolated to obtain the tangential velocities and these are then substituted into Eq. (12), a finite difference streamfield equation results. This finite difference equation is not the central difference form given by Eq. (17).

Adjacent to a boundary such as  $x = 0$  (Fig. 2a), the tangential velocity on the  $x = \Delta x/2$  face of the grid volume is the same as that used for the adjacent interior grid volume. Other velocities for the boundary element are evaluated from the boundary conditions. For the case of a rigid, no-slip surface at  $x = 0$ , the appropriate boundary conditions are  $u_{0,j} = v_{0,j} = 0$ . The tangential velocity  $u_{0,j}^t$  appearing in Fig. 2b is evaluated at the midheight ( $x = \Delta x/4$ ) of the vertical face by using a Taylor series expansion:

$$u_{0,j}^t = u_{0,j+1/2} + \left(\frac{\partial u}{\partial x}\right)_{0,j+1/2} \cdot \left(\frac{\Delta x}{4}\right) + O(\Delta x)^2.$$

The subscripts on the right side denote spatial locations. The first two terms on the right are found to be zero by applying the continuity equation and the velocity boundary conditions. Substitution of the appropriate velocities into Eq. (13) gives

$$\zeta_{0,j} = -2(\psi_{1,j} - \psi_{0,j})/r_j(\Delta x)^2. \quad (18)$$

Although this expression is second-order correct for the mean vorticity in the grid volume, it is only first order when applied to obtain boundary vorticity. Nevertheless, it is the only expression that is consistent with the interior vorticity field, thus allowing the circulation theorem to be satisfied. Various higher-order approximations are discussed by Orszag and Israeli [4] but these forms do not

satisfy the circulation theorem. Analysis similar to that above shows that at a free boundary

$$\zeta_{0,j} = 0 \tag{19}$$

to the same order of accuracy as Eq. (18).

Along the axis  $r = 0$  (Fig. 2b), an analogous procedure is applied to obtain the area-averaged vorticity. The appropriate velocity boundary conditions are  $\partial u/\partial r = v = 0$ . Consider first the tangential velocity  $v_{i,0}^t$  on the horizontal face  $x + \Delta x/2$ . Using a Taylor's series expansion for  $v_{i,0}^t$  evaluated at the midpoint of the face ( $r = \Delta r/4$ ), together with the continuity equation and the boundary conditions, gives

$$v_{i,0}^t = -(1/2)(\partial u/\partial x)_{i+1/2,0} (\Delta r/4) + O(\Delta r)^3. \tag{20}$$

Consider next the tangential velocities on the vertical faces,  $u_{i,0}^t$  and  $u_{i,0}$ . The  $\partial u/\partial r = 0$  boundary condition can be satisfied in either of two equivalent ways: by equating  $u_{i,0}^t$  and  $u_{i,0}$ , or by using Eq. (15a) for  $u_{i,0}^t$  and a two-point difference approximation for  $u_{i,0} = (\partial^2 \psi/\partial r^2)_{i,0}$ . Introducing these velocities into Eq. (14), the lowest-order terms cancel, giving

$$\zeta_{i,0} = -\frac{\Delta r}{4} \left[ \left( \frac{\partial^2 u}{\partial r^2} \right)_{i,0} + \frac{1}{2} \left( \frac{\partial^2 u}{\partial x^2} \right)_{i,0} \right]. \tag{21}$$

This expression is second-order correct for the area-averaged vorticity in the grid volume and also can be obtained by evaluating a Taylor's series for  $\zeta$  at the center of the grid volume. Setting the axis vorticity to zero

$$\zeta_{i,0} = 0 \tag{22}$$

satisfies Eq. (21) to first order and is consistent with the circulation theorem.

*Normal Velocity Components and Conservation of Mass*

For an incompressible fluid, mass or volume conservation is satisfied when the normal velocity components (transport velocities) appearing in Eq. (9) are defined in such a way that the volume source term  $Q_{i,j}$  is identically zero. It is convenient to introduce streamfunction values  $\psi_{i,j}^*$ , located at the corners of the grid volumes as shown in Fig. 1. In terms of the  $\psi^*$  values, as yet undefined, we define transport velocities as

$$u_{i,j}^n = (\psi_{i,j}^* - \psi_{i,j-1}^*)/r_j \Delta r \tag{23a}$$

$$v_{i,j}^n = (\psi_{i,j}^* - \psi_{i-1,j}^*)/(r_j + (\Delta r/2)) \Delta x. \tag{23b}$$



Substitution of these expressions into Eq. (9) confirms that volume flow is conserved. Along the axis with  $\psi = 0$  at  $r = 0$ , volume flow is conserved by taking

$$u_{i,0}^n = 2\psi_{i,0}^*/(\Delta r/2)^2. \quad (24)$$

The  $\psi^*$ -field is defined as a weighted average of the streamfunction at the four surrounding gridpoints

$$\psi_{i,j}^* = \alpha_j \left( \frac{\psi_{i,j} + \psi_{i+1,j}}{2} \right) + \beta_j \left( \frac{\psi_{i,j+1} + \psi_{i+1,j+1}}{2} \right). \quad (25)$$

This expression has been specialized to cylindrical coordinates by introducing two weighting coefficients  $\alpha_j$ ,  $\beta_j$ , and taking them to be uniform in the axial direction. In general, four coefficients depending on two coordinates may be introduced.

The essential step in our analysis is in determining the  $\alpha$ ,  $\beta$  coefficients by imposing a set of consistency conditions. These require the transport velocity to approach the gridpoint velocity (Eq. (16)) as the mesh is refined. That is

$$\left. \begin{aligned} |u_{i,j}^n - u_{i,j}| &\sim 0 \\ |v_{i,j}^n - v_{i,j}| &\sim 0 \end{aligned} \right\} \Delta x, \Delta r \rightarrow 0. \quad (26a)$$

$$(26b)$$

In the cylindrical geometry, radius is defined as  $r_j = j\Delta r$ , and two limits are possible as  $\Delta r$  is refined. One limit is found by holding  $r_j$  fixed, the second by holding  $j$  fixed.

Combining Eqs. (15), (16), (23), and (25), two expressions for the transport velocities may be obtained after some manipulation, as

$$v_{i,j}^n = \alpha_j \left( \frac{r_j}{r_j + \Delta r/2} \right) v_{i,j} + \beta_j \left( \frac{r_j + \Delta r}{r_j + \Delta r/2} \right) v_{i,j+1},$$

$$\begin{aligned} u_{i,j}^n = & \left\{ \alpha_j \psi_{i,j} + \beta_j \psi_{i,j+1} - \alpha_{j-1} \psi_{i,j-1} - \beta_{j-1} \psi_{i,j} \right. \\ & \left. + \left[ (\alpha_j - \beta_{j-1}) \left( \frac{\partial \psi}{\partial x} \right)_{i,j} + \beta_j \left( \frac{\partial \psi}{\partial x} \right)_{i,j+1} - \alpha_{j-1} \left( \frac{\partial \psi}{\partial x} \right)_{i,j-1} \right] \frac{\Delta x}{2} \right\} / r_j \Delta r. \end{aligned}$$

The first of these expressions will satisfy the consistency condition (26) for both radial limits if

$$\alpha_j + \beta_j = 1. \quad (27)$$

At fixed  $r_j$ , as  $\Delta r \rightarrow 0$ ,  $v_{i,j}$  approaches  $v_{i,j+1}$ ; whereas at fixed  $j$ , both  $v_{i,j}$  and  $v_{i,j+1}$  approach zero. The expression for  $u_{i,j}^n$  has been obtained by substituting Eq. (25) into Eq. (23a) and expanding in a Taylor's series about  $x = i\Delta x$ . For

purposes of analysis, the resulting expression is substituted into Eq. (26a) along with the expanded equation for the gridpoint velocity (Eqs. (16a) plus (15a)).

$$u_{i,j} = \left[ \frac{1}{1 + (\Delta r / (2r_j))} (\psi_{i,j+1} - \psi_{i,j}) + \frac{1}{1 - (\Delta r / (2r_j))} (\psi_{i,j} - \psi_{i,j-1}) \right] / 2r_j \Delta r.$$

For the limit of fixed  $r_j$ ,  $\Delta r \rightarrow 0$ , Eq. (26a) is satisfied if  $\alpha_j = \beta_j = 1/2$ . On the other hand, for the limit of fixed  $j$ ,  $\Delta r \rightarrow 0$ , we find that the recursion relation

$$\beta_j = \frac{1 + (2j - 1) \beta_{j-1}}{2j + 1} \tag{28}$$

is the weakest condition that will satisfy the limit. In obtaining the recursion formula the relation  $\psi \propto r^2$  has been used near the axis. For grid volumes on the axis,  $j = 0$ , we apply Eqs. (24) and (25) with  $\psi = 0$  at  $r = 0$  to obtain  $\beta_0 = 1/4$ . With  $\psi = 0$  at  $r = 0$ , the value  $\alpha_0$  need not be defined, but we take  $\alpha_0 = 3/4$  to agree with Eq. (27).

The sequence of  $\alpha_j$ ,  $\beta_j$  values described above is tabulated in Table I. The sequence of values for large  $j$ , obtained from the limit of fixed  $j$ ,  $\Delta r \rightarrow 0$ , approaches the value obtained from the limit of fixed  $r_j$ ,  $\Delta r \rightarrow 0$ . Transport velocities defined in this way conserve volume flow exactly and are consistent with the gridpoint velocity field as the mesh is refined.

TABLE I  
Weighting Coefficients Appearing in Eq. (22) and Defined by Eqs. (27) and (28)

$j$	$\alpha_j$	$\beta_j$
0	3/4	1/4
1	7/12	5/12
2	11/20	9/20
3	15/28	13/28
4	19/36	17/36
5	23/44	21/44
6	27/52	25/52
$\infty$	1/2	1/2

Summarizing the kinematically consistent formulation of velocity fields, the gridpoint velocities ( $u_{i,j}$ ,  $v_{i,j}$ ) given by Eq. (16) provide an approximation of the fluid velocity field, and the transport velocities ( $u_{i,j}^n$ ,  $v_{i,j}^n$ ) approximate the convective fluxes for a grid volume. The transport velocities conserve mass flow for each grid volume. The tangential velocity field ( $u_{i,j}^t$ ,  $v_{i,j}^t$ ) does not explicitly appear

in the finite difference calculations, but provides the connecting link between the gridpoint velocities and the finite difference streamfield equation by way of the circulation theorem. Thus, the vorticity-streamfunction relations are uniquely defined. Approximations other than Eq. (18) for boundary vorticity, for example, would be inconsistent. Transport velocities are related to grid point velocities by the consistency conditions of Eq. (26). The grid point and transport velocities defined in this way are kinematically consistent in the sense that conservation of mass and the circulation theorem are simultaneously satisfied by the finite difference approximations.

#### APPLICATION TO THERMAL CONVECTION

Finite difference approximations of the transport equations are solved using a forward time difference with a conserving upwind differencing of the convection terms and central differencing of the diffusion terms. The streamfield equation is approximated by Eq. (17), and the kinematically consistent velocities are used. To obtain steady-state solutions, time is treated as an iteration parameter. The time derivative is retained in the vorticity equation and the vorticity field is advanced simultaneously with the temperature field. The largest stable time step is used at each gridpoint to maximize the rate of iterative convergence locally. This procedure is analogous to Jacobi iteration. For certain ranges of parameters, Gauss-Seidel iteration of the energy equation has been used to speed convergence. The transport equations are advanced over a time step and the streamfield is iterated to convergence by optimized successive overrelaxation. Boundary conditions are then applied to update boundary temperature and boundary vorticity, completing the advancement. Other methods also have been applied to problems of this type. Houston and DeBraemaker [2] discuss application of the ADI method.

The physical problem including boundary conditions and the viscosity law is representative of thermal convection in the mantle of the earth. The complete base of the enclosure is at unit temperature, the vertical outer boundary is adiabatic, and the top is at zero temperature. The vertical outer boundary and base are free surfaces (no shear), while the top boundary is rigid (no-slip). The normalized kinematic viscosity is given by

$$\nu = \exp\{B(1 + Cx)/(1 + D\theta)\} \quad (29)$$

where values of the coefficients  $B$ ,  $C$ , and  $D$  are chosen to represent flow due to diffusion creep in the mantle. The coefficient  $C$  is negative and  $D$  is positive so that viscosity decreases as either height ( $x$ ) or temperature increase.

Isotherms, streamlines, and contours of constant viscosity are given in Fig. 3 for a steady-state flow with  $Ra = 10^6$ ,  $B = 54.10$ ,  $C = -0.326$ , and  $D = 0.484$ . A nonuniform spatial mesh was employed; the spacing is shown with tick marks along the edge of the enclosure. The strong dependence of viscosity on temperature and depth causes the flow to concentrate near the top and axis of the enclosure. Large velocity gradients appear in this region and it is here that nonphysical results occur with nonconsistent velocities.

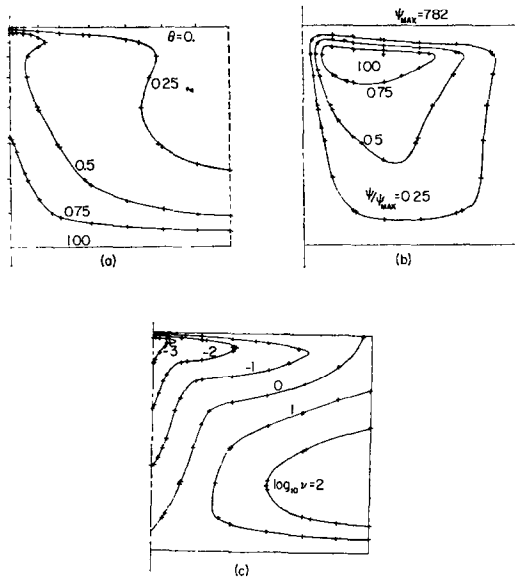


FIG. 3. Steady-state thermal convection with large viscosity variations,  $Ra = 10^6$ . (a) Isotherms. (b) Streamlines. (c) Contours of constant viscosity.

Anomalies are clearly apparent in the temperature field. Radial temperature distributions near the top boundary (one  $\Delta x$  below the top) are shown in Fig. 4. Figs. 4a and 4b present results for nonconsistent velocities. The results of Fig. 4b employ a more refined mesh than those of Fig. 4a. The off-axis temperature peak is strictly nonphysical. For these cases the axial velocity at gridpoints near the axis also shows an off-axis peak. Refining the mesh reduces the relative magnitude of the off-axis temperature peak and further refinement should eliminate the anomalies. However, the relatively slow rate of convergence for flows with strongly variable viscosity makes the use of more refined meshes undesirable. This is particularly true since we are more interested in approximate solutions over a wide range of physical conditions than in a few precise solutions at specific conditions.

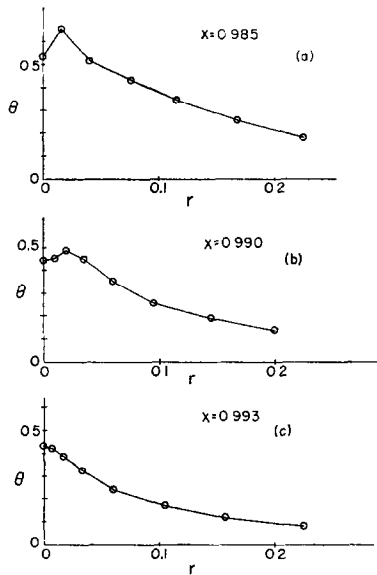


FIG. 4. Radial temperature distributions near the top boundary for steady state thermal convection with large viscosity variations,  $Ra = 10^5$ . (a) and (b) Inconsistent velocity fields. (c) Consistent velocity fields.

The anomalous behavior shown in Figs. 4a and 4b is caused by both the failure of difference approximations to conserve volume flow and their failure to satisfy the circulation theorem. Solutions have been obtained with conserving transport velocities, but with gridpoint velocities given by Eq. (7) (which are inconsistent with the circulation theorem and a central difference form of the streamfield equation). These results show no anomalies in the temperature field, but do show an off-axis peak of the axial velocity. Fig. 5c shows results using consistent velocities. This result, in contrast to cases a and b, shows no anomalous behavior of the temperature or axial velocity.

## CONCLUSIONS

Kinematically consistent finite difference approximations have been developed for velocity fields in cylindrical coordinates. These velocity fields allow volume flow to be conserved and the circulation theorem to be identically satisfied both locally and globally and lead to the familiar central difference form of the streamfield equation. When combined with the transport equations, which also conserve both locally and globally, a fully conserving finite difference approximation results.

Consistent velocity fields have been applied to thermal convection with highly variable viscosity. The consistent velocity fields are essential to obtaining physically correct solutions. Physical anomalies result from the failure of velocities to satisfy the kinematic conditions imposed by volume flow conservation and the circulation theorem. Although the present treatment has been specialized to cylindrical coordinates, the approach is readily generalized to other curvilinear coordinate systems. In Cartesian coordinates, the velocity approximations reduce to familiar central difference forms.

#### ACKNOWLEDGMENT

This work has been supported by the National Science Foundation under Grant GA-35075.

#### REFERENCES

1. J. E. FROMM, in "Methods in Computational Physics," Vol. 3, p. 345, Academic Press, New York, 1964.
2. M. W. HOUSTON AND J. CL. DE BRAEMAKER, *J. Comp. Phys.* **16** (1974), 221.
3. S. F. LIANG, A. VIDAL, AND A. ACRIVOS, *J. Fluid Mech.* **36** (1969), 239.
4. S. A. ORSZAG AND M. ISRAELI, *Ann. Rev. Fluid Mech.* **6** (1974), 281.
5. E. M. PARMENTIER, D. L. TURCOTTE, AND K. E. TORRANCE, *J. Geophys. Res.* (1975), in press.
6. K. E. TORRANCE, *J. Res. of Nat. Bur. Stand. USA* **72B** (1968), 281.
7. D. L. TURCOTTE, K. E. TORRANCE, AND A. T. HSUI, in "Methods in Computational Physics," Vol. 13, p. 431, Academic Press, New York, 1973.